Solid State Nuclear Magnetic Resonance 98 (2019) 1–11

Contents lists available at ScienceDirect

Solid State Nuclear Magnetic Resonance

journal homepage: www.elsevier.com/locate/ssnmr

Hyperpolarized MAS NMR of unfolded and misfolded proteins

Anna König [a,b], Daniel Schölzel [a,b], Boran Uluca [a,b], Thibault Viennet [a,b], Ümit Akbey [a,b], Henrike Heise [a,b,*]

[a] Institute of Complex Systems, Structural Biochemistry (ICS-6), Research Center Jülich, 52425, Jülich, Germany
[b] Institute of Physical Biology, Heinrich-Heine-University Düsseldorf, Universitätsstraße 1, 40225, Düsseldorf, Germany

ARTICLE INFO

Keywords:
Dynamic nuclear polarization
Intrinsically disordered proteins
Amyloid fibrils
Conformational ensemble
Frozen solution
Solid-state NMR

ABSTRACT

In this article we give an overview over the use of DNP-enhanced solid-state NMR spectroscopy for the investigation of unfolded, disordered and misfolded proteins. We first provide an overview over studies in which DNP spectroscopy has successfully been applied for the structural investigation of well-folded amyloid fibrils formed by short peptides as well as full-length proteins. Sample cooling to cryogenic temperatures often leads to severe line broadening of resonance signals and thus a loss in resolution. However, inhomogeneous line broadening at low temperatures provides valuable information about residual dynamics and flexibility in proteins, and, in combination with appropriate selective isotope labeling techniques, inhomogeneous linewidths in disordered proteins or protein regions may be exploited for evaluation of conformational ensembles. In the last paragraph we highlight some recent studies where DNP-enhanced MAS-NMR-spectroscopy was applied to the study of disordered proteins/protein regions and inhomogeneous sample preparations.

1. Introduction

The “native fold” of every protein which is invariably determined by its primary sequence has been a central paradigm of structural biology. However, this notion has lost its unrestricted validity by the notion that (i) a large class of proteins, the intrinsically disordered proteins (IDPs) do not possess one stable globular fold but exhibit many local minima and thus are highly flexible [1] and (ii) by the fact that most proteins are able to adopt alternative “misfolded” β-sheet rich conformations which all share a common structural cross-β motif [2].

Intrinsically disordered proteins are characterized by their high degree of conformational freedom which is due to a rather flat free energy landscape, comprising low energy barriers and many local minima. These allow IDPs to fluctuate rapidly over an ensemble of conformations in solution, instead of adopting a well-defined three-dimensional structure. Essential biological processes rely on IDPs, e.g. molecular recognition between kinases and substrates, transcription factors and effectors, etc. IDPs make up to 33% of eukaryotic proteins [3]; furthermore, many well-folded proteins in their native structure contain intrinsically disordered or highly flexible parts or domains in addition to the well-folded domains. The function of an IDP is thus not linked to one globular structure, but rather to a full ensemble of conformations, and a lot of effort has been made in trying to elucidate structural ensembles of IDPs [1,3,4].

Amyloid fibrils are involved in a large number of (neuro)degenerative diseases, such as Parkinson's disease, Alzheimer's disease and type-II diabetes. The misfolding of intrinsically disordered or globular proteins finally leads to the deposition of insoluble protein plaques which mainly consist of long, unbranched amyloid fibrils. Amyloid fibrils share certain structural features irrespective of their primary sequence. However, details of the amino acid residues involved in the cross-β-core region, the relative arrangement and registry of β-strands as well as the supramolecular and the macroscopic arrangement are not only determined by the amino acid sequence, but also depend critically on the exact fibrillation conditions. Thus, amyloid fibrils often exhibit a high degree of structural polymorphism. The central structural motif of amyloid fibrils is a cross β-pattern with β-strands perpendicular to the fiber axis. Intermolecular hydrogen bonds as well as hydrophobic and polar interactions between the amino acid side chains contribute to the high stability and robustness of amyloid fibrils. Amyloid formation occurs not only in protein misfolding diseases; indeed, amyloid fibers in bacteria, fungi, insects, invertebrates and humans also play functional roles (i.e. functional amyloids) [5]. Prominent examples of functional amyloids are yeast prions like HET-s, Ure2p and Sup35p, which are involved in horizontal gene transfer, as well as curli or TasA proteins, which stabilize the extracellular matrix of bacterial biofilms [6].

* Corresponding author. Institute of Complex Systems, Structural Biochemistry (ICS-6), Research Center Jülich, 52425, Jülich, Germany.
E-mail address: h.heise@fz-juelich.de (H. Heise).

https://doi.org/10.1016/j.ssnmr.2018.12.003
Received 28 September 2018; Received in revised form 28 December 2018; Accepted 30 December 2018
Available online 3 January 2019

The structural characterization of disordered and misfolded proteins is of paramount importance; however, both types of proteins pose a challenge on classical structural biology. The preferred technique for protein structure determination, X-ray crystallography, provides information about well-defined crystalline proteins, and flexible or disordered domains are invisible. Solution NMR spectroscopy on the other hand can only be applied to rather small (<100 kDa) proteins or complexes and is therefore not applicable for larger protein assemblies such as oligomers and protein aggregates. For IDPs, the structural characterization is even more complex, as not only one well-defined conformation, but rather a full conformational ensemble has to be determined. Chemical shifts and residual dipolar couplings in NMR are sensitive to conformational sampling. However, the exact observation of the conformational ensemble is prevented by rapid conformational averaging on the NMR time scale, and conformational distributions in many cases can be detected only indirectly. Nevertheless, it has recently been shown that solution NMR in combination with molecular dynamics simulations can be useful for the study of conformational ensembles of proteins [4].

Solid-state NMR-spectroscopy has lately proven its potential for structural characterization and even high-resolution structure determination of amyloid fibrils and other highly ordered multimeric protein assemblies (for recent reviews see Refs. [7–11], for some selected recent illustrative examples, see Refs. [12–16]). Very recent improvements in resolution obtainable by cryo electron microscopy (cryoEM) have enabled this method for structure determination in non-crystalline ordered protein assemblies, and first amyloid structures have been determined with the help of cryoEM (for selected examples, see Refs. [17–19]), thus improving our understanding of amyloid structures. In disordered or heterogeneous systems, NMR resonance assignment and unambiguous determination of structural constraints may be compromised by inhomogeneous line broadening. Solid-state NMR-spectroscopy at cryogenic temperatures – with or without DNP-enhancement – has been demonstrated to be a viable alternative for the study of intrinsically unfolded proteins or of protein preparations with high degree of conformational heterogeneity: At cryogenic temperatures, residual conformational averaging is prevented and different conformations are frozen out on the NMR timescale [20–22], and as a consequence, resonance lines are broadened [23,24]. However, these inhomogeneously broadened line-shapes contain information about the full conformational ensemble, which can be retrieved if the spectral overlap is reduced by adequate sparse isotope labeling techniques. The protein concentration in frozen solutions is often low, and sensitivity may further be compromised by the line broadening. Low sensitivity due to limited protein concentrations however can nowadays conveniently be overcome by dynamic nuclear polarization (DNP); thus, DNP-enhanced solid-state NMR-spectroscopy is becoming a viable tool to study not only well-ordered systems but also molecular assemblies with a high degree of structural disorder.

In the following article, we will first give a brief historical overview over DNP with a focus on biological applications. For more comprehensive reviews on DNP-enhanced biomolecular solid-state NMR-spectroscopy the reader is referred to the following recent excellent reviews [25–30]. In the second paragraph we will present a selection of examples where DNP-enhanced solid-state NMR-spectroscopy has successfully been applied to investigate well-ordered amyloid fibrils. We limit our overview to amyloid fibrils, but also other multimeric assemblies like intact viruses or capsids [31–33], bacterial secretion systems [34,35] or cell walls [36] have been studied by DNP-enhanced NMR-spectroscopy. For an excellent overview over these studies the reader is referred to a recent review by Jaudzems et al. [30].

In the last paragraph, we give an overview over studies where DNP-enhanced solid-state NMR-spectroscopy has been applied to the study of intrinsically disordered proteins or flexible regions of globular proteins or protein complexes as well as oligomers.

2. Historical overview

The phenomenon of Dynamic Nuclear Polarization (DNP) was first proposed theoretically by Overhauser in 1953 [37,38] and shortly after proved experimentally by Carver and Slichter in metallic Lithium. The general concept of DNP is the transfer of polarization from electrons to nuclei [39]. The originally proposed so-called Overhauser effect is based on T_1 cross-relaxation in a system of dipolar coupled electron-nuclear spins. It was then followed by the conceptual development of other DNP mechanisms: the solid effect by Ferries [40], the cross effect (CE) by Hwang and Hill [41,42], and the thermal mixing effect by Borghini [43]. These different DNP polarization mechanisms mainly depend on paramagnetic resonance properties of the electrons (EPR line-shape) and its magnitude relative to the nuclear Larmor frequency (ω_n) and matching conditions with the nuclei to be polarized (see Table 1).

In an ideal case, the exchange of magnetization between electrons and nuclei is proportional to the ratio of their energy population differences and thus to their gyromagnetic ratios. Therefore, the theoretical maximum enhancement or increase in nuclear magnetization is $|\gamma_e/\gamma_H| = 657$ for ^{1}H and $|\gamma_e/\gamma_C| = 2615$ for ^{13}C. In reality, however, the efficiency of the polarization transfer depends strongly on the T_1 relaxation time of the electron spins. For this reason, DNP is inefficient at high temperatures when fast tumbling rates lead to short electron T_1 relaxation times [44]. Moreover, successful saturation of the electron transition (in the microwave frequency range) is normally required in order to favor the transfer of magnetization from electron to nuclei. All these have three implications: (i) for efficient DNP the samples have to be cooled down to very low temperatures (usually around 100 K), (ii) frozen samples do not tumble and thus use of solid-state NMR is required and (iii) microwave irradiation has to reach the sample requiring special instrumentation [45].

It was more than 40 years later that the concept could be successfully applied to biomolecules after pioneering work of Griffin and coworkers [46–50]. Especially, this was due to the development of stable high frequency microwave sources (gyrotron) delivering resonant microwaves to the high field NMR spectrometers. Notably, this enabled investigation of the photocycle of the protein bacteriorhodopsin [51,52]. The increased sensitivity as well as the fact that the ^{15}N Schiff-base signal of a lysine residue (covalently bound to the retinal cofactor) is well isolated in chemical shift allowed its characterization.

A critical aspect of conducting DNP-enhanced NMR experiments is the choice of adequate polarization sources containing unpaired electrons, like stable organic radicals or transition metal complexes. For most biological applications nitroxide-based (i.e. TEMPO) radicals are used because of their good solubility and stability. For polarization enhancement via the cross effect, biradicals carrying two unpaired electrons of favorable properties have been shown to be very efficient. The TEMPO-based biradical TOTAPOL [53] has long been the compound of choice for cross effect DNP, now succeeded by the better performing AMUPol [54] with an increased longitudinal relaxation time of the electrons. As the EPR linewidth increases linearly with the magnetic field, the enhancement factor obtainable by CE DNP scales inversely with B_0. Therefore, mixed biradicals consisting of a nitroxide moiety with a large g-factor anisotropy and a trityl or BDPA radical with an almost isotropic g-factor are advantageous for CE DNP at high magnetic fields above 14 T [55–57]. Likewise, computationally designed asymmetric bis-nitroxides with large exchange interactions between the electrons where a parallel orientation of the nitroxide units is avoided, have been proven to favor efficient MAS DNP, and also polarizing agents containing two high-spin transition metal complexes are promising candidates for DNP-enhancement [58]. At magnetic fields above 14 T in combination with fast MAS rates, the solid Overhauser effect may become an attractive alternative to CE DNP [59–61]. This solid Overhauser effect is particularly effective at high magnetic fields for narrow line radicals with strong hyperfine interactions, like BDPA.

Another critical point is sample preparation. The radicals used, their

Table 1
Summary of DNP mechanisms' characteristics under MAS conditions (ω_{MW}, frequency of microwave irradiation; ω_e, electron Larmor frequency; ω_n, nuclear Larmor frequency; δ, electron transition homogeneous line broadening; Δ, electron transition inhomogeneous line broadening; d_{ee}, electron-electron distance; θ_{ee}, electron-electron angle, D_{ee}, electron-electron dipolar coupling constant).

Mechanism	Condition	Field dependence	Microwave requirement	Radical properties
Solid Overhauser effect	$\omega_{MW} = \omega_e$	Scales with B_0	Lower power < 2 W	Narrow EPR linewidth, strong hyperfine couplings Short T_{1e}
Solid effect	$\omega_n > \delta, \Delta$ $\omega_{MW} = \omega_e \pm \omega_n$	Scales with B_0^{-2}	Higher power	Narrow EPR line width
Cross effect	$\delta < \omega_n < \Delta$ $\omega_{e1} - \omega_{e2} = \omega_n$	Scales with B_0^{-1}	$\omega_{MW} = \omega_e$ Lower power	Broad EPR linewidth, biradical with fixed d_{ee} and θ_{ee}
Thermal mixing	$\omega_n < \delta$	Scales with B_0^{-1}	$\omega_{MW} = \omega_e$ Lower power	Broad EPR line High radical concentration or large D_{ee}

concentration and their localization throughout the sample are important factors. Optimization of these parameters is a sample dependent procedure and needs to be done individually. While conventional radicals are dissolved in the solvent together with the sample to obtain a statistical distribution and homogeneous hyperpolarization throughout the sample, other approaches using localized [62–65], covalently bound [66–70] or targeted [71,72] radicals are also possible. This presents several advantages such as better handling of paramagnetic relaxation enhancement (PRE) effects resulting from interactions with the unpaired electrons and access to specific information, and it is an interesting approach for the study of proteins in their native environments. Also, as phase separation and clustering of radicals, which may occur during ice crystal formation of water, is avoided, using cryoprotectants like glycerol is not always necessary (e.g. in presence of lipids). Particularly in the case of liposome-reconstituted membrane proteins, matrix-free sample preparation (i.e. a sample preparation in which the use of solvents is not necessary to enable a uniform distributions of polarizing agents) has proven to yield better relaxation properties leading to better signal per unit time [70,73]. Alternatively, sedimentation of proteins in the presence of free radicals leads to the formation of a glassy matrix at low temperatures and is thus an interesting alternative approach for sample preparation without the need for cryoprotectants [74,75]. Note that more or less specific interactions of globular proteins [65,75] and amyloid fibrils [76] with radicals have been shown. Thus, care has to be taken when sensitivity or resolution is compared between samples or regions of a sample.

One main advantage of DNP is its ability to enhance signals which would otherwise lie below the detection limit. The sensitivity enhancement can be attributed to the lowered temperature, causing a favorable Boltzmann distribution, and the microwave mediated polarization transfer from electrons to the nuclei. However, although the sensitivity might be vastly enhanced, the resolution is often drastically diminished under DNP conditions: Caused by the low temperatures, conformational averaging is mostly prevented, and water molecules are not uniformly distributed anymore. Furthermore, homogeneous line broadening due to paramagnetic relaxation enhancement and insufficient proton decoupling adds to the linewidth, a contribution which is particularly pronounced at low magnetic fields and moderate spinning speeds [33]. For uniformly isotope labeled samples the resolution after freezing may therefore not be sufficient. This can be counterbalanced by segmental and/or site-specific, amino-acid specific or sparse isotope labeling to reduce spectral crowding. As an example, in Fig. 1 two homonuclear $^{13}C,^{13}C$ correlation DNP spectra of globular 117-residue protein at a temperature of 110 K are displayed. While for the uniformly ^{13}C-labeled sample most resonances are overlapped so strongly that even a discrimination of signals from different amino acids is not possible anymore, in a spectrum of a protein uniformly ^{13}C labeled only for Isoleucine, different cross-correlation peaks can clearly be identified.

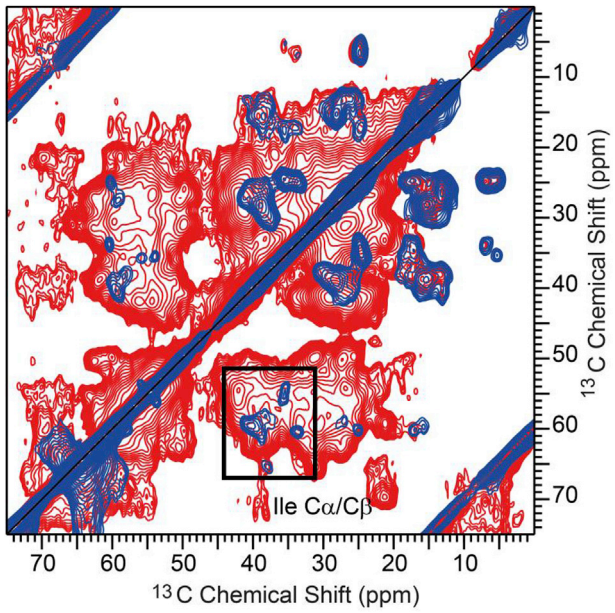

Fig. 1. Effect of amino acid-selective isotope labeling: Homonuclear 2D $^{13}C,^{13}C$ correlation spectra (acquired with proton driven spin diffusion with a mixing time of 10 ms at a field strength of 14.1 T with a spinning frequency of 9 kHz) of the 117-residue protein GABARAP in frozen solution. In the spectrum of the uniformly ^{13}C-labeled protein (red), signal crowding prevents the assignment of individual cross-peaks, whereas in the spectrum of the sample in which only the seven Isoleucine residues are uniformly ^{13}C labeled (blue), individual cross-correlation signals can be identified.

3. DNP-enhanced MAS NMR of amyloid fibrils

Amyloid fibrils, despite being the end product of protein misfolding and despite being prone to polymorphism, are often remarkably well-ordered. Valuable information about structural organization of amyloid fibrils has been obtained by conventional solid-state MAS NMR-spectroscopy [7–11]. In favorable cases full 3D structures were determined by solid-state NMR-spectroscopy and – very recently – also by cryo-EM [12–17,19]. In the following section we will focus on studies involving DNP-enhanced NMR-spectroscopy.

Many small peptide fragments of large amyloidogenic proteins are able to form amyloid fibrils. Although secondary structure elements as well as supramolecular structures of such peptide fibrils usually differ substantially from those of fibrils from full-length proteins, peptide fibrils are still valuable model systems enlightening fundamental principles of amyloid formation. One major advantage of chemically synthesized peptides over recombinantly expressed proteins for structure determination is the possibility to introduce isotope labels at any desired position in a site-selective manner.

One of the shortest fibril forming peptides is the seven amino acid residues segment GNNQQNY corresponding to amino acid residues 7 to

13 of the yeast prion Sup35p (vide infra) [77,78]. This peptide can not only form amyloid fibrils, but it can also crystallize into monoclinic and orthorhombic nanocrystals suitable for high-resolution X-ray crystallography. Substantial differences between nanocrystals and fibrils have been identified by solid-state NMR-spectroscopy [78]. Monoclinic crystals of this peptide were used as model systems to study the polarization transfer mechanism between solvent and sample. The tight packing of the peptide molecules within the crystal lattice excludes the bulky TOTAPOL biradicals from the sample. Thus, polarization enhancement of the peptide relies on ^{1}H polarization transfer by ^{1}H-^{1}H spin diffusion across the interface between the glassy solvent matrix and the sample [79]. Despite the rather large crystal dimensions of ~100–200 nm, an enhancement factor corresponding to 75% of the enhancement factor obtained for the solvent matrix was observed, suggesting that nanocrystals with a size of up to 1 μm can be efficiently hyperpolarized by DNP.

The correlation between sample dimensions and DNP-enhancement was further investigated by a comparison of enhancement factors obtained for fibril and crystal samples [80](*). Although the radical concentration in the fibril sample was substantially lower than in the crystal sample, polarization transfer by proton-driven spin diffusion was more efficient for the fibril. Since the rather thin fibrils with a diameter of a few nanometers facilitate closer contacts to the paramagnetic centers, polarization build-up was twice as fast as for the thicker crystals. At low temperatures, longitudinal mixing and build-up rates are enhanced, because dynamics are severely restricted resulting in greater efficiency for dipolar transfers. For fibrils, no significant chemical shift changes between high and low-temperature spectra were observed, while in monoclinic crystals sample freezing resulted in shift changes of up to 1.5 ppm for ^{13}C and 5 ppm for ^{15}N resonances, as well as to severe line broadening. Residues in close contact with water are most affected by shift changes and inhomogeneous line broadening.

A similar study focused on the complete architecture of an amyloid fibril formed by an 11 amino acid residue peptide segment of the transthyretin protein (TTR (105–115)) [81](*) [82]. The 3D structure of the peptides within the fibrils had been determined previously with high resolution by room temperature solid-state NMR-spectroscopy, demonstrating that the full peptide adopts an extended β-strand conformation [83,84]. With the help of DNP-enhanced solid-state NMR spectroscopy, intermolecular as well as intra- and inter-sheet contacts could be obtained on a set of ten different site-selectively isotope labeled samples in a fraction of the conventional measurement time (see Fig. 2 A). In detail, it could be shown that the fibrils are constructed by parallel in-register β-sheets. Furthermore, distance measurements between adjacent β-sheets indicated an anti-parallel arrangement of the sheets within the protofilaments in which odd-numbered side chains from peptides of one β-sheet are packed against even-numbered side chains from the other β-sheet. Thus, peptides in the two β-sheets are not equivalent, a fact which leads to resonance doubling in the NMR spectra. Supporting cryo-EM measurements identified three classes of fibrils consisting of four, six or eight protofilaments (Fig. 2B–D) [82]. Protofilament-to-protofilament contacts were shown to be organized in a head-to-tail fashion by distance measurements between single labels positioned at the N- and the C-terminus of the peptides.

DNP-enhanced solid-state NMR-spectroscopy was also successfully applied to determine the supramolecular arrangement in amyloid fibrils from larger proteins. In contrast to short model peptides which can conveniently be obtained by solid-phase synthesis, proteins with more than 40 to 50 residues usually are expressed recombinantly from *E. coli*, and thus different isotope labeling strategies are necessary to elucidate the supramolecular arrangement (which requires the measurement of long-distance restraints). In uniformly [^{13}C,^{15}N] labeled samples, the acquisition of these restraints is hampered by dipolar truncation effects. To overcome this problem, sparse or differential labeling as achieved e.g. by using 2-^{13}C glucose as sole carbon source in combination with DNP can be an appropriate choice: If fibrils are grown from a 1:1 mixture of sparsely [^{13}C,^{14}N] and [^{12}C,^{15}N] labeled monomers, only intermolecular

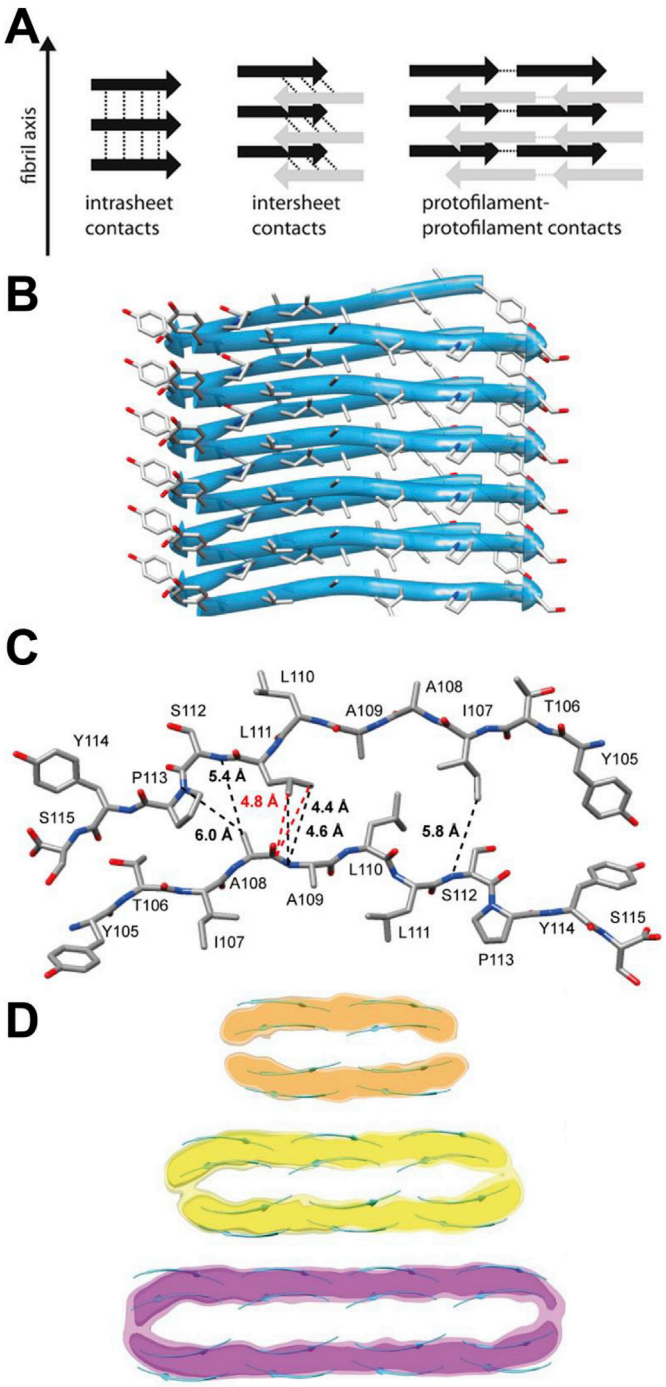

Fig. 2. A) Sketch of interstrand (intrasheet), intersheet and protofilament-to-protofilament contacts within amyloid fibrils. B) Side view and C) top view of one protofilament, composed of two TTR (105–115) peptide molecules. D) Three different fibril types composed of four, six and eight protofilaments, respectively. A-C) adapted with permission from Ref. [81], copyright (2013) American Chemical Society. D) adapted with permission from Ref. [82], copyright (2013) National Academy of Sciences.

contacts are detected in 2D ^{15}N/^{13}C correlation experiments, which in the case of in-register parallel arrangement of β-strands superimpose with intramolecular NCACX spectra of a uniformly labeled sample. For such experiments, signal enhancement by DNP, which boosts the sensitivity on lower gamma nuclei, is extremely helpful. Furthermore, local dynamics which at room temperature might attenuate the desired cross-peak intensities are frozen out at the low temperatures required for DNP, so long-

range polarization transfer efficiency is drastically improved.

This differential [^{13}C,^{15}N] isotope labeling approach has been successfully applied to confirm the parallel in-register alignment of β-strands in amyloid fibrils formed from an 86-residue protein, the PI3-SH3 domain, which is able to form highly ordered fibrils [85](*). Intermolecular N—C contacts in differentially [^{13}C,^{15}N] labeled fibrils were indicative of a parallel in-register alignment of the β-strands. Moreover, the parallel alignment was also corroborated from homonuclear long-range contacts from 2D ^{13}C/^{13}C correlation spectra of a sample sparsely ^{13}C labeled from 2-^{13}C-glucose. At long mixing times pseudo-intraresidual cross correlation signals between neighboring carbon atoms for which ^{13}C labeling occurs statistically, but for which simultaneous ^{13}C labeling within one amino acid residue is not possible, could be observed. This supports a structural alignment in which equivalent amino acid residues are in close proximity to each other.

Another challenging amyloid fibril studied by DNP-enhanced solid-state NMR spectroscopy is the yeast prion protein Sup35p [86], a translation termination factor with an N-terminal prion domain which is able to convert into a self-propagating amyloid form, which leads to sequestration of the protein together with a loss-of-function phenotype. The full-length protein has 684 amino acid residues and is composed of an N-terminal prion domain (called N) rich in uncharged polar residues N and Q, a C-terminal translation termination domain and a highly charged middle domain (M) which connects the latter and provides solubility. The 263 amino acids long fragment SupNM consisting of the N- and M-domain is sufficient to form amyloid fibrils that can transmit the prion phenotype to yeast colonies [87]. Fibrils of Sup35NM have been studied by various groups using solid-state NMR-spectroscopy, however, a converging structural model is still elusive due to the inherent propensity of Sup35p to form different polymorphs associated with different prion strains and also due to high conformational inhomogeneity [88–90]. The exact length and location of the amyloid core has been found to depend on the fibrillation temperature [89] or on the prion strain [90] and may also be influenced by the presence or absence of the C-terminal domain. Furthermore, a second putative amyloid core region has been identified in a single point mutant of Sup35NM [91]. Due to substantial inhomogeneous line broadening as well as considerable spectral overlap resulting from an unfavorable amino acid composition, site-selective resonance assignment was not possible for most of the resonances. Only 22 amino acid residues located N-terminal of position 30 gave rise to extremely well-resolved signals and could be sequentially assigned from 3D triple-resonance spectra [88]. However, signals from less ordered parts of the protein were also visible in the spectrum. Even if a resonance assignment was not possible, these signals could – in combination with site-selective isotope labeling and dedicated recoupling techniques – still be exploited to determine the supramolecular arrangement of these less structured protein regions: A large portion of the amino acids in the N-domain was found to be located in parallel in-register β-sheets [92], albeit less well-structured than the beginning of the N-terminus.

Frederick et al. applied DNP-enhanced solid-state NMR spectroscopy to further study Sup35NM fibrils in a cellular environment by using a cell lysate of yeast cells exhibiting the strong prion phenotype as fibrillation medium for recombinantly expressed [^{13}C,^{15}N], isotope labeled Sup35NM [93](*). In contrast to purified fibrils generated by seeded fibrillation in lysis buffer the fibrils obtained from cell lysates were found to have significantly higher β-sheet content. In particular, signals of residues which are exclusively located in the dynamically disordered M-domain were better defined in the lysate-grown fibrils, a fact which may be explained by specific interactions of this part of the protein with cellular components such as heat shock proteins. In a second study, Frederick et al. investigated the supramolecular arrangement of Sup35NM fibrils by combining sparse differential [^{15}N/^{13}C] labeling with segmental labeling. With the help of the split-intein technology, it was possible to express Sup35NM protein where only the first 14 residues are isotope labeled. Uniform [^{15}N/^{13}C] labeling of these 14 residues enabled full sequential resonance assignment. Chemical shifts for the ^{7}GNNQQN^{13}Y fragment differ substantially from the corresponding shifts obtained in microcrystals as well as in all fibril types formed by this peptide fragment alone [78]. Thus, the conformation of this amino acid stretch in full-length fibrils clearly differs from that found in fibrils formed by the model peptide. To probe the supramolecular arrangement of the monomers, fibrils were also grown from a mixture of monomers with different isotope labeling: half of the monomers were uniformly [^{15}N] labeled, for the other half of the monomers, only the first 14 amino acid residues were sparsely [^{13}C] labeled [94](*). ^{15}N/^{13}C correlation spectra obtained with long TEDOR transfer did not superimpose with short range TEDOR spectra obtained on fibrils sparsely [^{13}C] and uniformly [^{15}N] labeled for these first 14 residues, a result which would be expected for parallel β-sheets with in-register alignment. This finding indicates that at least not all of the first 14 amino acid residues are part of an antiparallel β-sheet in the fibrils used for this study.

The impact of low temperatures on spectral resolution has been investigated without DNP-enhancement using amyloid fibrils of Aβ(1–40) [95] as well as of HET-s (218–289) [96] as model systems. For well-ordered Aβ(1–40) fibrils, the loss in resolution at low temperatures was moderate at a high static magnetic field of 20 T (corresponding to a proton Larmor frequency of 850 MHz), thus suggesting that conformational heterogeneity in this sample is not limiting the resolution [95]. A similar study, notably in absence of radicals and without the addition of the cryoprotectant glycerol, has been conducted on HET-s (218–289) fibrils at a magnetic field strength of 14.1 T (600 MHz proton Larmor frequency). 2D ^{13}C/^{13}C correlation spectra were acquired at different temperatures ranging from 100 to 280 K. The overall resolution of the ^{13}C NMR-spectra decreases gradually and monotonously with decreasing temperatures, similar as observed for a microcrystalline protein [97]. Resonances from residues in the well-structured hydrophobic core of the fibril are still reasonably resolved at low temperatures, whereas most hydrophilic amino acid residues pointing to the outside of the fibril were broadened beyond detectability upon freezing of the surrounding water shell.

In a similar way, amyloid fibrils formed by human islet amyloid polypeptide IAPP showed inhomogeneous line broadening at low temperatures. While the linewidth of most residues was affected by low temperatures, this effect was particularly pronounced for the seven N-terminal residues which form a loop bridged by a disulfide bond between Cys2 and Cys7 [98]. Signals from these residues were also broadened beyond detectability at low temperatures, an effect which may be attributed to increased intrinsic flexibility of this part of the peptide.

Finally, aggregates involved in bacterial virulence, such as curli (CsgA aggregates), may form amyloid fibrils as well. The biradical TOTAPOL shows a high binding affinity to the amyloid surface of CsgA fibrils, similar to the affinity of the fluorescent dye Thioflavin T (ThT) [76](*). Both molecules share a similar molecular framework and rotational symmetry, which allows them to bind to ridges formed by protruding side chains on the fibrillar surface. As a result, polarization is directly transferred via strong couplings between nitroxide radicals and the nuclear spins at the fibril surface. To achieve a balanced ratio between optimizing the sensitivity while avoiding paramagnetic relaxation enhancement and bleaching effects, the radical concentration has to be decreased (~400 fold), compared to commonly employed concentrations of around 10–20 mM.

In summary, with the help of DNP-enhanced solid-state NMR-spectroscopy valuable structural information on well-ordered protein assemblies may be obtained. Although cryogenic temperatures may cause line broadening and a decrease in resolution, the reduced mobility and increased signal-to noise ratio may enable the observation of several long-range contacts which are otherwise inaccessible by traditional solid-state NMR-spectroscopy. Further, residual line broadening at lower temperatures correlates well with residual flexibility and is thus another important source of information.

4. DNP-enhanced MAS NMR of disordered proteins

Besides the investigation of well-ordered systems with the help of (DNP-enhanced) solid-state NMR, solid-state NMR at cryogenic temperatures (with or without DNP-enhancement) is also a powerful method for obtaining information on disordered or heterogeneous systems, such as unstructured parts of bigger assemblies, intrinsically disordered proteins, or on heterogeneous systems like oligomers. At cryogenic temperatures, the full structural ensemble of an unfolded or partially folded protein is freeze-trapped, and thus the full conformational ensemble may be evaluated by solid-state NMR spectroscopy. The structural ensemble obtained by freeze trapping critically depends on the freezing conditions: if the cooling rate is slower than the time scale for structural rearrangements, the equilibrium conformational ensemble at the temperature of glass formation is obtained. Rapid freezing on time scales much faster than the time scale of conformational averaging on the other hand enables the trapping of transient intermediates and allows in principle to follow protein folding processes [99]. Further, to prevent cold denaturation by ice crystal formation, the addition of cryoprotectants is mandatory. While MAS NMR of frozen solutions at cryogenic temperatures is now possible, freeze-trapped preparation may also be lyophilized in order to stabilize the trapped ensemble state [100].

Chemical shifts in general and secondary chemical shifts of backbone atoms Cα and Cβ in particular are sensitive signatures of the protein conformation and the secondary structure. In principle, secondary structure elements reflect the backbone conformation of the protein, which can be represented as a pair of backbone torsion angles on the Ramachandran plot (Fig. 3A), and different regions of the Ramachandran plot give rise to distinct secondary chemical shifts [101]. In globular proteins with defined backbone fold, accurate predictions on secondary structure elements can be made based on secondary chemical shifts. In disordered proteins or protein regions, on the other hand, typical "random coil chemical shifts" are observed. These random coil shifts do not correspond to a defined "random coil backbone conformation" represented by a distinct area on the Ramachandran plot, but they are the result of rapid averaging over all energetically favored conformations (Fig. 3A and B). If the sample is frozen, all conformations sampled by the protein are present in the sample with their respective probability. As a consequence, every protein conformation gives rise to different chemical shifts, and the resonance lines are thus broadened (Fig. 3C). These inhomogeneously broadened line shapes can in principle be evaluated to obtain information on the relative contents of conformations typical for α-helical or β-sheet-like (extended) conformations [102–104].

Pioneering studies on protein folding of a 35 residue protein domain of the vilin headpiece by cryogenic solid-state NMR-spectroscopy have demonstrated the power of this method (reviewed in Ref. [20]). Equilibrium conformational ensembles of the chemically denatured ([102, 105]) protein domain could be quantified from studies of different site-selectively labeled peptides in frozen solution. Furthermore, rapid freezing from different temperatures above and below the thermal denaturation point allowed for the trapping of a transient folding intermediate [99] with secondary structure elements characteristic of the fully folded protein domain, but with a lower degree of sidechain order, which is an indication of a lack of tertiary structure in this intermediate.

The enhanced sensitivity of DNP makes it possible to study small peptides in large assemblies, which enables the investigation of proteins in environments similar to their natural environments. In this respect Lange et al. were able to study the disulfide oxidoreductase A (DsbA) secretion monitor (SecM) signaling peptide within the exit tunnel of the ribosome. To achieve this, the peptide was uniformly [$^{13}C/^{15}N$] labeled, whereas the ribosome was unlabeled. Additionally, in order to suppress natural abundance signals of unwanted species, 2D experiments were employed, because the probability of a cross peak of two correlating carbons is reduced by a factor of 100. Upon cooling to 105 K, the conformational states of DsbA-SecM have been studied, and in contrast to earlier studies, it has been shown that only a minor population of DsbA-SecM adopts an α-helical structure within the ribosome, thus demonstrating that protein folding may already occur during translation [106](*).

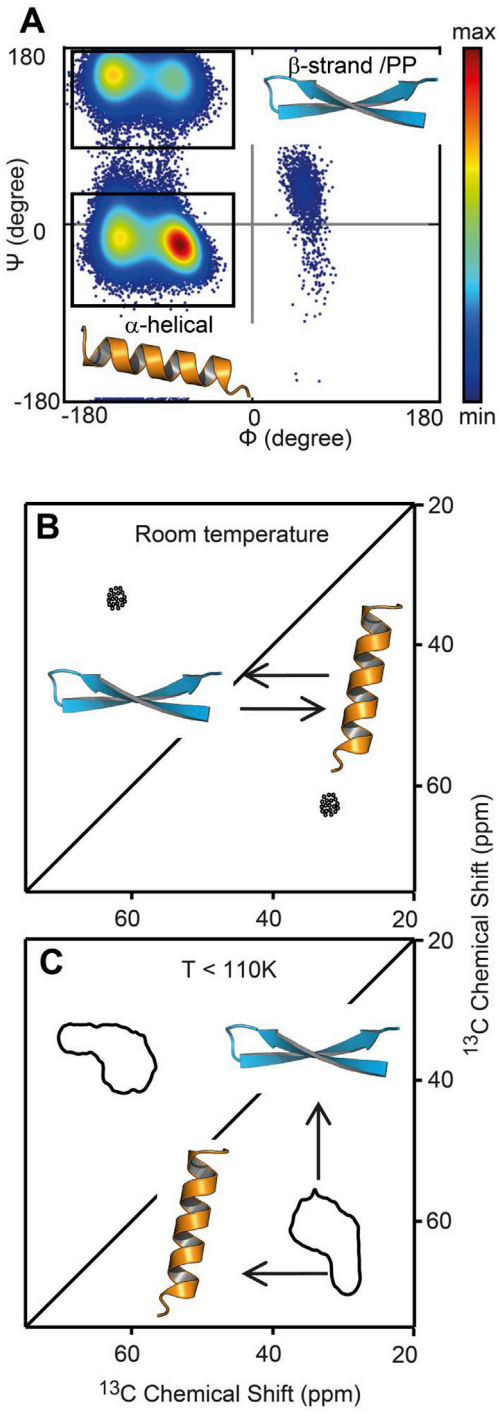

Fig. 3. A) Ramachandran plot displaying the probability distributions for backbone conformations of the residue Valine in an intrinsically disordered peptide. Regions for α-helical and β-strand/Polyproline conformations are indicated with boxes. B) Schematic representation of Cα/Cβ cross correlation peaks (for the amino acid Valine) with random coil chemical shifts in an intrinsically disordered protein. Random coil chemical shifts are averages caused by rapid transitions between α-helical and β-sheet like conformations. C) At low temperatures every molecule is frozen in a different conformation, and different backbone torsion angles in the conformational ensembles give rise to distinct chemical shifts, thus leading to inhomogeneous line broadening (see Ref. [104]). Adapted with permission from Ref. [104], copyright (2018) Elsevier.

Another example for the use of DNP to enhance signals of small peptides in a larger assembly is PL12, a silaffin-derived pentalysine peptide, which catalyzes the silicic acid condensation in vitro. This peptide was embedded in silica to model the cell-wall. An interesting fact of this study is that neither the silica matrix nor the peptide was isotope labeled. Nevertheless, ^{13}C CP-spectra could be obtained at a temperature of 100 K within minutes without major loss of resolution and with an enhancement factor of 30. This shows the unique ability of DNP to study even unlabeled peptides in a larger assembly. With the help of 2D heteronuclear correlation and double-quantum-single-quantum correlation spectra a change in backbone conformation inside the silica in comparison to free PL12 in solution could be detected [107].

The power of DNP to decipher structurally well-ordered and intrinsically disordered parts of proteins was also demonstrated by Gupta et al. The study of tubular capsids of different HIV-1 protein assemblies at different field strengths and temperatures allowed the analysis of line broadening effects in DARR-spectra. With increasing field strength the resolution could be significantly improved, which demonstrates that line broadening in DNP-spectra is not exclusively caused by inhomogeneous line broadening but also contains homogeneous contributions (which can be counterbalanced by high field strengths). The highly dynamic and disordered spacer peptide 1 could be identified and distinguished from the conformational homogeneous capsid proteins at cryogenic temperatures. Decreasing the temperature from 180 K to 109 K did not lead to any further loss in resolution. Moreover, it was possible to assign aromatic side chains in the spectra obtained at cryogenic temperatures, a task which is generally challenging at room temperature [32](*).

The protein α-synuclein is a chimeric protein, because it can adopt different structures in different environments. It is natively unfolded and disordered, but in the progress of Parkinson's disease it forms fibrils with a β-sheet rich core structure, and upon membrane-association it becomes predominantly α-helical. Nevertheless, even in the structured forms some parts remain unstructured and flexible exhibiting random coil chemical shifts. We investigated the conformational ensembles sampled by this protein in different environments with the help of DNP-enhanced solid-state NMR-spectroscopy. In order to reduce spectral crowding, the protein was sparsely isotope labeled by using 2-^{13}C-glucose as main carbon source and supplying ten amino acids in natural abundance to the growth medium [108]. With this labeling scheme, simultaneous ^{13}C labeling for neighboring Cα and Cβ positions occurs only in Valine residues, such that Cα/Cβ cross correlation signal of Valine may be exploited as a reporter for secondary structure at the Valine positions. At cryogenic temperatures (such as needed for DNP) the Cα/Cβ cross peak of all 19 Valine residues present in the protein separates into specific amounts of α-helical and β-strand content (see Fig. 4 A). We could show that it is possible to obtain information on the conformational ensemble by analyzing the line shapes of the corresponding peaks. In fibrillar (Fig. 4B) α-synuclein, the β-sheet content is increased, but residual intensity at chemical shifts indicative of α-helical conformations suggests that not only the highly charged C-terminus but also the first ~38 N-terminal residues are disordered, a finding which is in agreement with current structural models [12,109]. We also investigated the secondary structure of α-synuclein in the presence of lipid bilayers. By using nanodiscs as membrane mimetics we were able to exactly control the ratio between α-synuclein monomers and membrane surface [110]. As expected, a large part of the α-synuclein protein adopted α-helical conformation upon contact with lipid bilayers. The exact amount of helical conformation, however, strongly depended on the protein-to-lipid ratio. We could quantify the extent of the unstructured regions in different membrane-bound forms by comparing intensities of different parts of the cross-peak to those of the monomeric form. Increasing protein-to-lipid ratios resulted in larger disordered fractions of the protein, a finding which was also supported by solution NMR [110]. Furthermore, we demonstrated that consecutive residues have a strong tendency to adopt the same secondary structure (Fig. 4A), a finding which may be indicative of formation of transient secondary structure elements even in the disordered form [104](*).

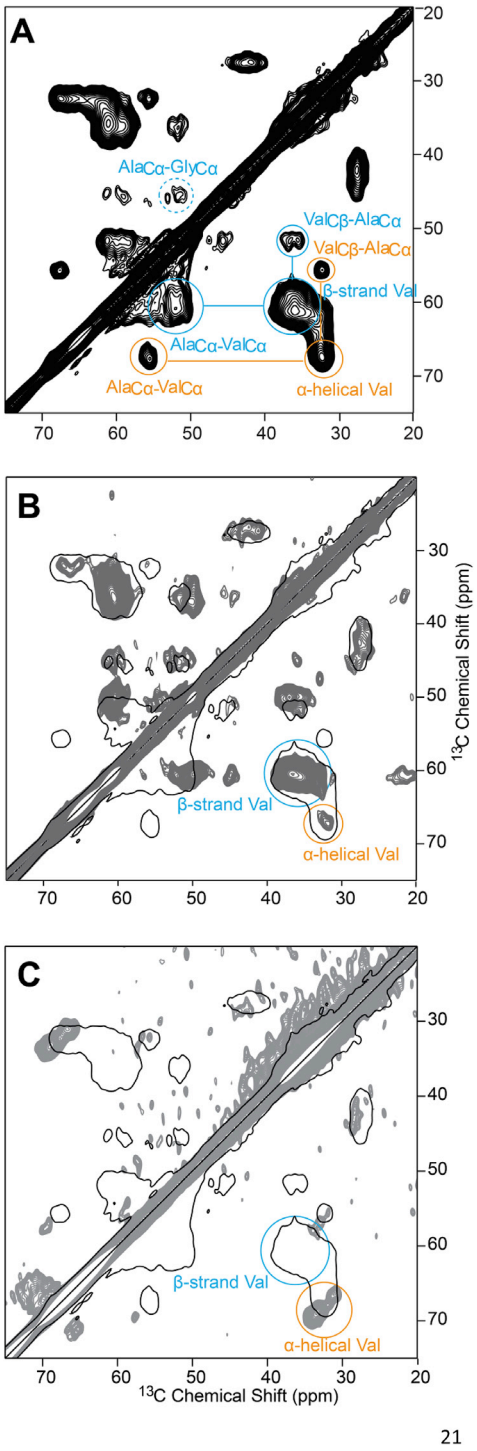

Fig. 4. 2D ^{13}C/^{13}C-correlation spectra (acquired with proton-driven spin-diffusion with a mixing time of 1 s, at a field strength of 14.1 T, with a spinning frequency of 9 kHz) of sparsely ^{13}C labeled α-synuclein in frozen solution in different environment. A) For disordered monomeric α-synuclein in a glycerol-water solution the Valine Cα/Cβ cross-correlation signal is largely inhomogeneously broadened, shift regions typical for α-helical as well as for β-strand like conformations are covered. Further, interresidual cross-correlation signals to neighboring Alanine residues are indicative of a correlation between similar conformations for neighboring residues. B) For a frozen suspension of fibrillar α-synuclein (grey spectrum) the β-sheet content is increased with respect to monomeric α-synuclein (black outline), whereas for α-synuclein in contact with lipid bilayers (C) only α-helical shifts are observed. Adapted with permission from Ref. [104], copyright (2018) Elsevier.

To our knowledge to date there is only one study on metastable, transient species using DNP. Potapov et al. measured DNP on different Aβ(1–40) species at different stages of the fibrillation pathway [111]. Samples were not lyophilized, but were measured in frozen solution. Thus the use of DNP was essential to obtain sufficient sensitivity. In total, four samples with different Aβ(1–40) species were investigated, the first containing primarily monomers, the second monomers and oligomers of different sizes and morphologies, the third metastable protofibrils and the fourth fibrils formed out of the protofibrils. With the help of 2D ^{13}C PDSD or DARR spectra extended β-sheet-like conformations could be identified in all samples, which are even predominant in the monomeric and oligomeric samples despite higher conformational disorder. Secondly, a close contact between F19 and L34 was observed in all four samples, indicating contacts between these two residues even before the development of structurally ordered assemblies. This contact is most pronounced in the protofibrils, which indicates a lower distance between F19 and L34 in protofibrils compared to fibrils. These findings reveal that the predominant molecular conformation is similar at all stages of fibrillation. Additionally, intermolecular ^{13}C spin polarization transfers between labeled carbonyl and aliphatic sites were measured. Aβ(1–40) protofibrils did not adopt an in-register, parallel β-sheet structure as in mature fibrils, i.e. Aβ(1–40) protofibrils are metastable 'off-pathway' intermediates with a more rapid nucleation [111](*).

Finally, the potential of DNP-enhanced solid-state NMR-spectroscopy has not only been applied to study disordered but isolated and purified proteins, but also to investigate proteins in their cellular environments, i.e. cell lysates [72,93,112–114] and whole cells [115–117]. For an extensive overview over the field of in-cell NMR-spectroscopy we refer to an excellent recent review by Luchinat and Banci [118] and limit ourselves here to highlighting one study in which localized DNP was used to site-selectively hyperpolarize the protein of interest [72](*). One of the main challenges of NMR-spectroscopy in cellular environments is the selective detection of NMR signals of the target protein in the presence of a large background of other cellular proteins and macromolecules. Most of the in-cell NMR studies solve this task either by injecting the fully [^{13}C,^{15}N] labeled target protein into cells grown in a growth medium with natural abundance isotope distribution or by overexpressing the target protein directly after adding isotope labeled precursors to the growth medium. Viennet et al. chose a different route to achieve selectivity by covalently attaching the biradical TOTAPOL to a binding partner of the target protein. With this approach it was possible to selectively hyperpolarize Bcl-x_L in non-purified cell lysates, in which the target protein as well as the background were uniformly [^{13}C, ^{15}N] labeled. However, the approach required an almost 100% deuteration level of the background in order to prevent extensive loss of polarization into the solvent. Since no purification and isotope labeling steps are required, the benefits of this approach might be a reduction of workload, sample loss and amount of needed isotopes.

5. Outlook

In this contribution we have demonstrated the broad range of applicability of DNP-enhanced solid-state NMR-spectroscopy to the investigation of unfolded and misfolded proteins, and the large potential of this technique also for structural biology. Recent improvements as well as ongoing research will further increase the application range of this method.

One of the limitations of DNP so far has been the loss of enhancement when increasing external magnetic fields. Nevertheless, recent development of cross effect radicals with more robust relaxation properties (TEKPol series) [119] and design of Overhauser methodologies applicable to MAS-NMR [59–61,120] enabled DNP studies up to 800 MHz, a field strength at which a reasonable resolution may be obtained. One main issue remains, i.e. the inhomogeneous line broadening of samples at very low temperatures with different conformations frozen out. While the homogeneous contribution to line broadening is field independent and as such can be counterbalanced by high magnetic fields, faster spinning rates and higher proton decoupling [33], the inhomogeneous contribution to the linewidth can mainly be overcome by increasing temperatures (shown as high-temperature DNP, [97]). This is of course possible but usually dramatic for the enhancement because electron longitudinal relaxation times become unfavorable for efficient DNP. Very recently, enhancements up to 15-fold at 200 K have been reported on biomolecules in conventional conditions using either deuterated proteins [121] or AMUPol/CD_3-TOTAPOL (note however that it is reported to be very sample-dependent) [122]. Homogeneous line broadening by paramagnetic relaxation enhancement on the other hand may successfully be reduced by decoupling of the electrons [123]. Furthermore, the application of pulsed microwave irradiation instead of continuous wave irradiation [124,125] may have significant advantages. For instance, very short hyperpolarization build-up times using electron spin-lock $T_{1\rho}$ build-up in the order of ns instead of the conventional T_1 build-up times of the order of seconds have been successfully carried out at 0.34 T (NOVEL experiment). Implementation of this at high fields would further push the limits of DNP-enhancement.

Acknowledgement

This work was supported by the DFG (HE 3243/4-1) and by the Ministry of Innovation, Science and Research within the framework of the NRW StrategieprojektBioSC (BioSc seed fund). T.V. acknowledges support from the International Graduate School of Protein Science and Technology (iGRASPseed) granted by the Ministry of Innovation, Science and Research of the state North Rhine-Westphalia. The authors gratefully acknowledge access to the Jülich-Düsseldorf Biomolecular NMR Center.

References

[1] P.E. Wright, H.J. Dyson, Intrinsically disordered proteins in cellular signalling and regulation, Nat. Rev. Mol. Cell Biol. 16 (1) (2015) 18–29.
[2] F. Chiti, C.M. Dobson, Protein misfolding, amyloid formation, and human disease: a summary of progress over the last decade, Annu. Rev. Biochem. 86 (1) (2017) 27–68.
[3] J.J. Ward, J.S. Sodhi, L.J. McGuffin, B.F. Buxton, D.T. Jones, Prediction and functional analysis of native disorder in proteins from the three kingdoms of life, J. Mol. Biol. 337 (3) (2004) 635–645.
[4] I.C. Felli, R. Pierattelli, Intrinsically Disordered Proteins Studied by NMR Spectroscopy, Springer, New York, 2015.
[5] D.M. Fowler, A.V. Koulov, W.E. Balch, J.W. Kelly, Functional amyloid - from bacteria to humans, Trends Biochem. Sci. 32 (5) (2007) 217–224.
[6] A. Diehl, Y. Roske, L. Ball, A. Chowdhury, M. Hiller, N. Molière, R. Kramer, D. Stöppler, C.L. Worth, B. Schlegel, M. Leidert, N. Cremer, N. Erdmann, D. Lopez, H. Stephanowitz, E. Krause, B.-J. van Rossum, P. Schmieder, U. Heinemann, K. Turgay, Ü. Akbey, H. Oschkinat, Structural changes of TasA in biofilm formation of *Bacillus subtilis*, Proc. Natl. Acad. Sci. Unit. States Am. 115 (13) (2018) 3237–3242.
[7] W. Hoyer, H. Heise, What does solid-state NMR tell us about amyloid structures? in: D. Otzen (Ed.), Amyloid Fibrils and Prefibrillar Aggregates Wiley-VCH Verlag GmbH & Co. KGaA, 2013, pp. 39–61.
[8] W. Hoyer, H. Shaykhalishahi, S. Ayalur-Karunakaran, H. Heise, Structural characterization of alpha-synuclein amyloids, in: The Prion Phenomena in Neurodegenerative Diseases: New Frontiers in Neuroscience, Nova Science Biomedical, 2015, pp. 111–128.
[9] R. Tycko, Molecular structure of aggregated amyloid-β: insights from solid state nuclear magnetic resonance, Cold Spring Harbor Perspect. Medi. 6 (8) (2016), https://doi.org/10.1101/cshperspect.a024083 a024083.
[10] B.H. Meier, R. Riek, A. Böckmann, Emerging structural understanding of amyloid fibrils by solid-state NMR, Trends Biochem. Sci. 42 (10) (2017) 777–787.
[11] P.C.A. van der Wel, Insights into protein misfolding and aggregation enabled by solid-state NMR spectroscopy, Solid State Nucl. Magn. Reson. 88 (Supplement C) (2017) 1–14.
[12] M.D. Tuttle, G. Comellas, A.J. Nieuwkoop, D.J. Covell, D.A. Berthold, K.D. Kloepper, J.M. Courtney, J.K. Kim, A.M. Barclay, A. Kendall, W. Wan, G. Stubbs, C.D. Schwieters, V.M.Y. Lee, J.M. George, C.M. Rienstra, Solid-state NMR structure of a pathogenic fibril of full-length human [alpha]-synuclein, Nat. Struct. Mol. Biol. 23 (5) (2016) 409–415.
[13] M.A. Wälti, F. Ravotti, H. Arai, C.G. Glabe, J.S. Wall, A. Böckmann, P. Güntert, B.H. Meier, R. Riek, Atomic-resolution structure of a disease-relevant Aβ(1–42) amyloid fibril, Proc. Natl. Acad. Sci. Unit. States Am. 113 (34) (2016) E4976–E4984.
[14] M.T. Colvin, R. Silvers, Q.Z. Ni, T.V. Can, I. Sergeyev, M. Rosay, K.J. Donovan, B. Michael, J. Wall, S. Linse, R.G. Griffin, Atomic resolution structure of

monomorphic Aβ42 amyloid fibrils, J. Am. Chem. Soc. 138 (30) (2016) 9663–9674.
[15] D.T. Murray, M. Kato, Y. Lin, K.R. Thurber, I. Hung, S.L. McKnight, R. Tycko, Structure of FUS protein fibrils and its relevance to self-assembly and phase separation of low-complexity domains, Cell 171 (3) (2017), 615-627.e16.
[16] C. Wasmer, A. Lange, H. Van Melckebeke, A.B. Siemer, R. Riek, B.H. Meier, Amyloid fibrils of the HET-s(218-289) prion form a β−Solenoid with a triangular hydrophobic core, Science 319 (5869) (2008) 1523–1526.
[17] A.W.P. Fitzpatrick, B. Falcon, S. He, A.G. Murzin, G. Murshudov, H.J. Garringer, R.A. Crowther, B. Ghetti, M. Goedert, S.H.W. Scheres, Cryo-EM structures of tau filaments from Alzheimer's disease, Nature 547 (7662) (2017) 185–190.
[18] B. Falcon, W. Zhang, A.G. Murzin, G. Murshudov, H.J. Garringer, R. Vidal, R.A. Crowther, B. Ghetti, S.H.W. Scheres, M. Goedert, Structures of filaments from Pick's disease reveal a novel tau protein fold, Nature 561 (7721) (2018) 137–140.
[19] L. Gremer, D. Schölzel, C. Schenk, E. Reinartz, J. Labahn, R.B.G. Ravelli, M. Tusche, C. Lopez-Iglesias, W. Hoyer, H. Heise, D. Willbold, G.F. Schröder, Fibril structure of amyloid-β(1–42) by cryo–electron microscopy, Science 358 (6359) (2017) 116–119.
[20] K.-N. Hu, R. Tycko, What can solid state NMR contribute to our understanding of protein folding? Biophys. Chem. 151 (1–2) (2010) 10–21.
[21] A.B. Barnes, B. Corzilius, M.L. Mak-Jurkauskas, L.B. Andreas, V.S. Bajaj, Y. Matsuki, M.L. Belenky, J. Lugtenburg, J.R. Sirigiri, R.J. Temkin, J. Herzfeld, R.G. Griffin, Resolution and polarization distribution in cryogenic DNP/MAS experiments, Phys. Chem. Chem. Phys. 12 (22) (2010) 5861–5867.
[22] A.H. Linden, W.T. Franks, U. Akbey, S. Lange, B.J. van Rossum, H. Oschkinat, Cryogenic temperature effects and resolution upon slow cooling of protein preparations in solid state NMR, J. Biomol. NMR 51 (3) (2011) 283–292.
[23] D.L. Jakeman, D.J. Mitchell, W.A. Shuttleworth, J.N. Evans, Effects of sample preparation conditions on biomolecular solid-state NMR lineshapes, J. Biomol. NMR 12 (3) (1998) 417–421.
[24] A.B. Siemer, K.Y. Huang, A.E. McDermott, Protein linewidth and solvent dynamics in frozen solution NMR, PLoS One 7 (10) (2012), e47242.
[25] Y. Su, L. Andreas, R.G. Griffin, Magic angle spinning NMR of proteins: high-frequency dynamic nuclear polarization and 1H detection, Annu. Rev. Biochem. 84 (1) (2015) 465–497.
[26] A.S. Lilly Thankamony, J.J. Wittmann, M. Kaushik, B. Corzilius, Dynamic nuclear polarization for sensitivity enhancement in modern solid-state NMR, Prog. NMR Spectrosc. 102–103 (2017) 120–195.
[27] U. Akbey, H. Oschkinat, Structural biology applications of solid state MAS DNP NMR, J. Magn. Reson. 269 (2016) 213–224.
[28] E.J. Koers, E.A. van der Cruijsen, M. Rosay, M. Weingarth, A. Prokofyev, C. Sauvee, O. Ouari, J. van der Zwan, O. Pongs, P. Tordo, W.E. Maas, M. Baldus, NMR-based structural biology enhanced by dynamic nuclear polarization at high magnetic field, J. Biomol. NMR 60 (2–3) (2014) 157–168.
[29] J.H. Ardenkjaer-Larsen, G.S. Boebinger, A. Comment, S. Duckett, A.S. Edison, F. Engelke, C. Griesinger, R.G. Griffin, C. Hilty, H. Maeda, G. Parigi, T. Prisner, E. Ravera, J. van Bentum, S. Vega, A. Webb, C. Luchinat, H. Schwalbe, L. Frydman, Facing and overcoming sensitivity challenges in biomolecular NMR spectroscopy, Angew. Chem., Int. Ed. Engl. 54 (32) (2015) 9162–9185.
[30] K. Jaudzems, T. Polenova, G. Pintacuda, H. Oschkinat, A. Lesage, DNP NMR of biomolecular assemblies, J. Struct.l Biol. (2019), https://doi.org/10.1016/j.jsb.2018.09.011 in press.
[31] I.V. Sergeyev, B. Itin, R. Rogawski, L.A. Day, A.E. McDermott, Efficient assignment and NMR analysis of an intact virus using sequential side-chain correlations and DNP sensitization, Proc. Natl. Acad. Sci. Unit. States Am. 114 (20) (2017) 5171–5176.
[32] (*) R. Gupta, M. Lu, G. Hou, M.A. Caporini, M. Rosay, W. Maas, J. Struppe, C. Suiter, J. Ahn, I.-J.L. Byeon, W.T. Franks, M. Orwick-Rydmark, A. Bertarello, H. Oschkinat, A. Lesage, G. Pintacuda, A.M. Gronenborn, T. Polenova, Dynamic nuclear polarization enhanced MAS NMR for structural analysis of HIV-1 protein assemblies, J. Chem. Phys. B 120 (2) (2016) 329–339.
* This work represents the DNP-enhanced NMR study of a large HIV-1 protein assembly. Additionally shows that the spectral line broadening effects have both homogeneous and inhomogeneous contributions.
[33] K. Jaudzems, A. Bertarello, S.R. Chaudhari, A. Pica, D. Cala-DePaepe, E. Barbet-Massin, A.J. Pell, I. Akopjana, S. Kotelovica, D. Gajan, O. Ouari, K. Tars, G. Pintacuda, A. Lesage, Dynamic nuclear polarization-enhanced biomolecular NMR spectroscopy at high magnetic field with fast magic-angle spinning, Angew. Chem. Int. Ed. 57 (25) (2018) 7458–7462.
[34] P. Fricke, J.P. Demers, S. Becker, A. Lange, Studies on the MxiH protein in T3SS needles using DNP-enhanced ssNMR spectroscopy, ChemPhysChem 15 (1) (2014) 57–60.
[35] P. Fricke, D. Mance, V. Chevelkov, K. Giller, S. Becker, M. Baldus, A. Lange, High resolution observed in 800 MHz DNP spectra of extremely rigid type III secretion needles, J. Biomol. NMR 65 (3) (2016) 121–126.
[36] T. Wang, Y.B. Park, M.A. Caporini, M. Rosay, L. Zhong, D.J. Cosgrove, M. Hong, Sensitivity-enhanced solid-state NMR detection of expansin's target in plant cell walls, Proc. Natl. Acad. Sci. U. S. A 110 (41) (2013) 16444–16449. S16444/1-S16444/12.
[37] A.W. Overhauser, Polarization of nuclei in metals, Phys. Rev. 92 (2) (1953) 411–415.
[38] T.R. Carver, C.P. Slichter, Polarization of nuclear spins in metals, Phys. Rev. 92 (1) (1953) 212–213.
[39] A.W. Overhauser, Paramagnetic relaxation in metals, Phys. Rev. 89 (4) (1953) 689–700.
[40] C.D. Jeffries, Polarization of nuclei by resonance saturation in paramagnetic crystals, Phys. Rev. 106 (1) (1957) 164–165.
[41] C.F. Hwang, D.A. Hill, New effect in dynamic polarization, Phys. Rev. Lett. 18 (4) (1967) 110–112.
[42] C.F. Hwang, D.A. Hill, Phenomenological model for the new effect in dynamic polarization, Phys. Rev. Lett. 19 (18) (1967) 1011–1014.
[43] M. Borghini, Spin-temperature model of nuclear dynamic polarization using free radicals, Phys. Rev. Lett. 20 (9) (1968) 419–421.
[44] K.-N. Hu, G.T. Debelouchina, A.A. Smith, R.G. Griffin, Quantum mechanical theory of dynamic nuclear polarization in solid dielectrics, J. Chem. Phys. 134 (12) (2011) 125105.
[45] M. Rosay, M. Blank, F. Engelke, Instrumentation for solid-state dynamic nuclear polarization with magic angle spinning NMR, J. Magn. Reson. 264 (2016) 88–98.
[46] G.J. Gerfen, L.R. Becerra, D.A. Hall, R.G. Griffin, R.J. Temkin, D.J. Singel, High frequency (140 GHz) dynamic nuclear polarization: polarization transfer to a solute in frozen aqueous solution, J. Chem. Phys. 102 (24) (1995) 9494.
[47] D.A. Hall, D.C. Maus, G.J. Gerfen, S.J. Inati, L.R. Becerra, F.W. Dahlquist, R.G. Griffin, Polarization-enhanced NMR spectroscopy of biomolecules in frozen solution, Science 276 (5314) (1997) 930–932.
[48] M. Rosay, A.C. Zeri, N.S. Astrof, S.J. Opella, J. Herzfeld, R.G. Griffin, Sensitivity-enhanced NMR of biological solids: dynamic nuclear polarization of Y21M fd bacteriophage and purple membrane, J. Am. Chem. Soc. 123 (5) (2001) 1010–1011.
[49] M. Rosay, V. Weis, K.E. Kreischer, R.J. Temkin, R.G. Griffin, Two-dimensional (13) C-(13)C correlation spectroscopy with magic angle spinning and dynamic nuclear polarization, J. Am. Chem. Soc. 124 (13) (2002) 3214–3215.
[50] M. Rosay, J.C. Lansing, K.C. Haddad, W.W. Bachovchin, J. Herzfeld, R.J. Temkin, R.G. Griffin, High-frequency dynamic nuclear polarization in MAS spectra of membrane and soluble proteins, J. Am. Chem. Soc. 125 (45) (2003) 13626–13627.
[51] M.L. Mak-Jurkauskas, V.S. Bajaj, M.K. Hornstein, M. Belenky, R.G. Griffin, J. Herzfeld, Energy transformations early in the bacteriorhodopsin photocycle revealed by DNP-enhanced solid-state NMR, Proc. Natl. Acad. Sci. U.S.A. 105 (3) (2008) 883–888.
[52] V.S. Bajaj, M.L. Mak-Jurkauskas, M. Belenky, J. Herzfeld, R.G. Griffin, Functional and shunt states of bacteriorhodopsin resolved by 250 GHz dynamic nuclear polarization-enhanced solid-state NMR, Proc. Natl. Acad. Sci. U. S. A 106 (23) (2009) 9244–9249. S9244/1-S9244/4.
[53] C. Song, K.N. Hu, C.G. Joo, T.M. Swager, R.G. Griffin, TOTAPOL: a biradical polarizing agent for dynamic nuclear polarization experiments in aqueous media, J. Am. Chem. Soc. 128 (35) (2006) 11385–11390.
[54] C. Sauvee, M. Rosay, G. Casano, F. Aussenac, R.T. Weber, O. Ouari, P. Tordo, Highly efficient, water-soluble polarizing agents for dynamic nuclear polarization at high frequency, Angew. Chem., Int. Ed. Engl. 52 (41) (2013) 10858–10861.
[55] G. Mathies, M.A. Caporini, V.K. Michaelis, Y. Liu, K.N. Hu, D. Mance, J.L. Zweier, M. Rosay, M. Baldus, R.G. Griffin, Efficient dynamic nuclear polarization at 800 MHz/527 GHz with trityl-nitroxide biradicals, Angew. Chem., Int. Ed. Engl. 54 (40) (2015) 11770–11774.
[56] D. Wisser, G. Karthikeyan, A. Lund, G. Casano, H. Karoui, M. Yulikov, G. Menzildjian, A.C. Pinon, A. Purea, F. Engelke, S.R. Chaudhari, D. Kubicki, A.J. Rossini, I.B. Moroz, D. Gajan, C. Copéret, G. Jeschke, M. Lelli, L. Emsley, A. Lesage, O. Ouari, BDPA-nitroxide biradicals tailored for efficient dynamic nuclear polarization enhanced solid-state NMR at magnetic fields up to 21.1 T, J. Am. Chem. Soc. 140 (41) (2018) 13340–13349.
[57] L.F. Pinto, I. Marín-Montesinos, V. Lloveras, J.L. Muñoz-Gómez, M. Pons, J. Veciana, J. Vidal-Gancedo, NMR signal enhancement of >50 000 times in fast dissolution dynamic nuclear polarization, Chem. Commun. 53 (26) (2017) 3757–3760.
[58] M. Kaushik, M. Qi, A. Godt, B. Corzilius, Bis-gadolinium complexes for solid effect and cross effect dynamic nuclear polarization, Angew. Chem., Int. Ed. Engl. 56 (15) (2017) 4295–4299.
[59] T.V. Can, M.A. Caporini, F. Mentink-Vigier, B. Corzilius, J.J. Walish, M. Rosay, W.E. Maas, M. Baldus, S. Vega, T.M. Swager, R.G. Griffin, Overhauser effects in insulating solids, J. Chem. Phys. 141 (6) (2014), 064202.
[60] M. Lelli, S.R. Chaudhari, D. Gajan, G. Casano, A.J. Rossini, O. Ouari, P. Tordo, A. Lesage, L. Emsley, Solid-state dynamic nuclear polarization at 9.4 and 18.8 T from 100 K to room temperature, J. Am. Chem. Soc. 137 (46) (2015) 14558–14561.
[61] S.R. Chaudhari, D. Wisser, A.C. Pinon, P. Berruyer, D. Gajan, P. Tordo, O. Ouari, C. Reiter, F. Engelke, C. Copéret, M. Lelli, A. Lesage, L. Emsley, Dynamic nuclear polarization efficiency increased by very fast magic angle spinning, J. Am. Chem. Soc. 139 (31) (2017) 10609–10612.
[62] C. Fernandez-de-Alba, H. Takahashi, A. Richard, Y. Chenavier, L. Dubois, V. Maurel, D. Lee, S. Hediger, G. De Paepe, Matrix-free DNP-enhanced NMR spectroscopy of liposomes using a lipid-anchored biradical, Chemistry 21 (12) (2015) 4512–4517.
[63] T. Maly, D. Cui, R.G. Griffin, A.F. Miller, 1H dynamic nuclear polarization based on an endogenous radical, J. Phys. Chem. B 116 (24) (2012) 7055–7065.
[64] A.N. Smith, M.A. Caporini, G.E. Fanucci, J.R. Long, A method for dynamic nuclear polarization enhancement of membrane proteins, Angew. Chem., Int. Ed. Engl. 54 (5) (2015) 1542–1546.
[65] H. Takahashi, I. Ayala, M. Bardet, G. De Paepe, J.P. Simorre, S. Hediger, Solid-state NMR on bacterial cells: selective cell wall signal enhancement and resolution improvement using dynamic nuclear polarization, J. Am. Chem. Soc. 135 (13) (2013) 5105–5110.

[66] E.A. van der Cruijsen, E.J. Koers, C. Sauvee, R.E. Hulse, M. Weingarth, O. Ouari, E. Perozo, P. Tordo, M. Baldus, Biomolecular DNP-supported NMR spectroscopy using site-directed spin labeling, Chemistry 21 (37) (2015) 12971–12977.
[67] V. Vitzthum, F. Borcard, S. Jannin, M. Morin, P. Mieville, M.A. Caporini, A. Sienkiewicz, S. Gerber-Lemaire, G. Bodenhausen, Fractional spin-labeling of polymers for enhancing NMR sensitivity by solvent-free dynamic nuclear polarization, ChemPhysChem 12 (16) (2011) 2929–2932.
[68] M.A. Voinov, D.B. Good, M.E. Ward, S. Milikisiyants, A. Marek, M.A. Caporini, M. Rosay, R.A. Munro, M. Ljumovic, L.S. Brown, V. Ladizhansky, A.I. Smirnov, Cysteine-specific labeling of proteins with a nitroxide biradical for dynamic nuclear polarization NMR, J. Phys. Chem. B 119 (32) (2015) 10180–10190.
[69] B.J. Wylie, B.G. Dzikovski, S. Pawsey, M. Caporini, M. Rosay, J.H. Freed, A.E. McDermott, Dynamic nuclear polarization of membrane proteins: covalently bound spin-labels at protein-protein interfaces, J. Biomol. NMR 61 (3–4) (2015) 361–367.
[70] E.S. Salnikov, S. Abel, G. Karthikeyan, H. Karoui, F. Aussenac, P. Tordo, B. Bechinger, O. Ouari, Dynamic nuclear polarization/solid-state NMR spectroscopy of membrane polypeptides: free-radical optimization for matrix-free lipid bilayer samples, ChemPhysChem 18 (15) (2017) 2103–2113.
[71] R. Rogawski, I.V. Sergeyev, Y. Li, M.F. Ottaviani, V. Cornish, A.E. McDermott, Dynamic nuclear polarization signal enhancement with high-affinity biradical tags, J. Phys. Chem. B 121 (6) (2017) 1169–1175.
[72] (*) T. Viennet, A. Viegas, A. Kuepper, S. Arens, V. Gelev, O. Petrov, T.N. Grossmann, H. Heise, M. Etzkorn, Selective protein hyperpolarization in cell lysates using targeted dynamic nuclear polarization, Angew. Chem., Int. Ed. Engl. 55 (36) (2016) 10746–10750.
* Approach for targeted and site-selective in-cell NMR spectroscopy in combination with DNP. By covalently attaching a radical to a ligand peptide, only the receptor for this ligand is selectively hyperpolarized.
[73] H. Takahashi, S. Hediger, G. De Paepe, Matrix-free dynamic nuclear polarization enables solid-state NMR 13C-13C correlation spectroscopy of proteins at natural isotopic abundance, Chem. Commun. (Camb) 49 (82) (2013) 9479–9481.
[74] E. Ravera, B. Corzilius, V.K. Michaelis, C. Rosa, R.G. Griffin, C. Luchinat, I. Bertini, Dynamic nuclear polarization of sedimented solutes, J. Am. Chem. Soc. 135 (5) (2013) 1641–1644.
[75] E. Ravera, B. Corzilius, V.K. Michaelis, C. Luchinat, R.G. Griffin, I. Bertini, DNP-enhanced MAS NMR of bovine serum albumin sediments and solutions, J. Phys. Chem. B 118 (11) (2014) 2957–2965.
[76] (*) M. Nagaraj, T.W. Franks, S. Saeidpour, T. Schubeis, H. Oschkinat, C. Ritter, B.J. van Rossum, Surface binding of TOTAPOL assists structural investigations of amyloid fibrils by dynamic nuclear polarization NMR spectroscopy, Chembiochem 17 (14) (2016) 1308–1311.
* A beautiful representation of the inverse effects of using large radical concentration in resolution. shows also that some radicals bind to fibrils, so there needs to be further optimization protocol for studying every single sample.
[77] R. Nelson, M.R. Sawaya, M. Balbirnie, A.O. Madsen, C. Riekel, R. Grothe, D. Eisenberg, Structure of the cross-[beta] spine of amyloid-like fibrils, Nature 435 (7043) (2005) 773–778.
[78] P.C.A. van der Wel, J.R. Lewandowski, R.G. Griffin, Solid-state NMR study of amyloid nanocrystals and fibrils formed by the peptide GNNQQNY from yeast prion protein Sup35p, J. Am. Chem. Soc. 129 (16) (2007) 5117–5130.
[79] P.C. van der Wel, K.N. Hu, J. Lewandowski, R.G. Griffin, Dynamic nuclear polarization of amyloidogenic peptide nanocrystals: GNNQQNY, a core segment of the yeast prion protein Sup35p, J. Am. Chem. Soc. 128 (33) (2006) 10840–10846.
[80] (*) G.T. Debelouchina, M.J. Bayro, P.C. van der Wel, M.A. Caporini, A.B. Barnes, M. Rosay, W.E. Maas, R.G. Griffin, Dynamic nuclear polarization-enhanced solid-state NMR spectroscopy of GNNQQNY nanocrystals and amyloid fibrils, Phys. Chem. Chem. Phys. 12 (22) (2010) 5911–5919.
* An in-depth investigation and analysis of DNP polarization transfer via spin diffusion into large peptide crystals and amyloid fibrils.
[81] (*) G.T. Debelouchina, M.J. Bayro, A.W. Fitzpatrick, V. Ladizhansky, M.T. Colvin, M.A. Caporini, C.P. Jaroniec, V.S. Bajaj, M. Rosay, C.E. MacPhee, M. Vendruscolo, W.E. Maas, C.M. Dobson, R.G. Griffin, Higher order amyloid fibril structure by MAS NMR and DNP spectroscopy, J. Am. Chem. Soc. 135 (51) (2013) 19237–19247.
* DNP NMR study focusing on the large-scale architecture of fibrils from an 11-residue peptide from transthyretin protein.
[82] A.W.P. Fitzpatrick, G.T. Debelouchina, M.J. Bayro, D.K. Clare, M.A. Caporini, V.S. Bajaj, C.P. Jaroniec, L. Wang, V. Ladizhansky, S.A. Müller, C.E. MacPhee, C.A. Waudby, H.R. Mott, A. De Simone, T.P.J. Knowles, H.R. Saibil, M. Vendruscolo, E.V. Orlova, R.G. Griffin, C.M. Dobson, Atomic structure and hierarchical assembly of a cross-β amyloid fibril, Proc. Natl. Acad. Sci. Unit. States Am. 110 (14) (2013) 5468–5473.
[83] C.P. Jaroniec, C.E. MacPhee, N.S. Astrof, C.M. Dobson, R.G. Griffin, Molecular conformation of a peptide fragment of transthyretin in an amyloid fibril, Proc. Natl. Acad. Sci. U. S. A 99 (26) (2002) 16748–16753.
[84] C.P. Jaroniec, C.E. MacPhee, V.S. Bajaj, M.T. McMahon, C.M. Dobson, R.G. Griffin, High-resolution molecular structure of a peptide in an amyloid fibril determined by magic angle spinning NMR spectroscopy, Proc. Natl. Acad. Sci. U. S. A 101 (3) (2004) 711–716.
[85] (*) M.J. Bayro, G.T. Debelouchina, M.T. Eddy, N.R. Birkett, C.E. MacPhee, M. Rosay, W.E. Maas, C.M. Dobson, R.G. Griffin, Intermolecular structure determination of amyloid fibrils with magic-angle spinning and dynamic nuclear polarization NMR, J. Am. Chem. Soc. 133 (35) (2011) 13967–13974.
* Application of different protein isotope labeling approaches to determine macromolecular arrangements within an amyloid fibril.
[86] J.R. Glover, A.S. Kowal, E.C. Schirmer, M.M. Patino, J.J. Liu, S. Lindquist, Self-seeded fibers formed by Sup35, the protein determinant of [PSI+], a heritable prion-like factor of S-cerevisiae, Cell 89 (5) (1997) 811–819.
[87] L. Li, S. Lindquist, Creating a protein-based element of inheritance, Science 287 (5453) (2000) 661–664.
[88] N. Luckgei, A.K. Schütz, L. Bousset, B. Habenstein, Y. Sourigues, C. Gardiennet, B.H. Meier, R. Melki, A. Böckmann, The conformation of the prion domain of Sup35 p in isolation and in the full-length protein, Angew. Chem. Int. Ed. 52 (48) (2013) 12741–12744.
[89] F. Shewmaker, D. Kryndushkin, B. Chen, R. Tycko, R.B. Wickner, Two prion variants of Sup35p have in-register parallel beta-sheet structures, independent of hydration, Biochemistry 48 (23) (2009) 5074–5082.
[90] Kendra K. Frederick, Galia T. Debelouchina, C. Kayatekin, T. Dorminy, Angela C. Jacavone, Robert G. Griffin, S. Lindquist, Distinct prion strains are defined by amyloid core structure and chaperone binding site dynamics, Chem. Biol. 21 (2) (2014) 295–305.
[91] Y. Ohhashi, Y. Yamaguchi, H. Kurahashi, Y.O. Kamatari, S. Sugiyama, B. Uluca, T. Piechatzek, Y. Komi, T. Shida, H. Müller, S. Hanashima, H. Heise, K. Kuwata, M. Tanaka, Molecular basis for diversification of yeast prion strain conformation, Proc. Natl. Acad. Sci. Unit. States Am. 115 (10) (2018) 2389–2394.
[92] A. Gorkovskiy, K.R. Thurber, R. Tycko, R.B. Wickner, Locating folds of the in-register parallel β-sheet of the Sup35p prion domain infectious amyloid, Proc. Natl. Acad. Sci. Unit. States Am. 111 (43) (2014) E4615–E4622.
[93] (*) K.K. Frederick, V.K. Michaelis, B. Corzilius, T.C. Ong, A.C. Jacavone, R.G. Griffin, S. Lindquist, Sensitivity-enhanced NMR reveals alterations in protein structure by cellular milieus, Cell 163 (3) (2015) 620–628.
* A beautiful representation of the power of structural biology by state-of-the-art DNP NMR, by sensitivity enhancement and proteins prepared in-vitro versus in cell lysate of the yeast prion Sup35NM.
[94] (*) K.K. Frederick, V.K. Michaelis, M.A. Caporini, L.B. Andreas, G.T. Debelouchina, R.G. Griffin, S. Lindquist, Combining DNP NMR with segmental and specific labeling to study a yeast prion protein strain that is not parallel in-register, Proc. Natl. Acad. Sci. U. S. A 114 (14) (2017) 3642–3647.
* Extension of work in ref.89, towards determination of more structural information. The study combines a crucial split-intein labeling technology, that converges structural possibilities from NMR distance restraints.
[95] J.M. Lopez del Amo, D. Schneider, A. Loquet, A. Lange, B. Reif, Cryogenic solid state NMR studies of fibrils of the Alzheimer's disease amyloid-beta peptide: perspectives for DNP, J. Biomol. NMR 56 (4) (2013) 359–363.
[96] T. Bauer, C. Dotta, L. Balacescu, J. Gath, A. Hunkeler, A. Bockmann, B.H. Meier, Line-broadening in low-temperature solid-state NMR spectra of fibrils, J. Biomol. NMR 67 (1) (2017) 51–61.
[97] U. Akbey, A.H. Linden, H. Oschkinat, High-temperature dynamic nuclear polarization enhanced magic-angle-spinning NMR, Appl. Magn. Reson. 43 (1–2) (2012) 81–90.
[98] F. Weirich, L. Gremer, E.A. Mirecka, S. Schiefer, W. Hoyer, H. Heise, Structural characterization of fibrils from recombinant human islet amyloid polypeptide by solid-state NMR: the central FGAILS segment is part of the β-sheet core, PLoS One 11 (9) (2016), e0161243.
[99] K.-N. Hu, W.-M. Yau, R. Tycko, Detection of a transient intermediate in a rapid protein folding process by solid-state nuclear magnetic resonance, J. Am. Chem. Soc. 132 (1) (2010) 24–25.
[100] S. Chimon, M.A. Shaibat, C.R. Jones, D.C. Calero, B. Aizezi, Y. Ishii, Evidence of fibril-like β-sheet structures in a neurotoxic amyloid intermediate of Alzheimer's β-amyloid, Nat. Struct. Mol. Biol. 14 (12) (2007) 1157–1164.
[101] B. Han, Y. Liu, S. Ginzinger, D. Wishart, SHIFTX2: significantly improved protein chemical shift prediction, J. Biomol. NMR 50 (1) (2011) 43–57.
[102] R.H. Havlin, R. Tycko, Probing site-specific conformational distributions in protein folding with solid-state NMR, Proc. Natl. Acad. Sci. U.S.A. 102 (9) (2005) 3284–3289.
[103] H. Heise, S. Luca, B.L. de Groot, H. Grubmüller, M. Baldus, Probing conformational disorder in neurotensin by two-dimensional solid-state NMR and comparison to molecular dynamics simulations, Biophys. J. 89 (3) (2005) 2113–2120.
[104] (*) B. Uluca, T. Viennet, D. Petrović, H. Shaykhalishahi, F. Weirich, A. Gönülalan, B. Strodel, M. Etzkorn, W. Hoyer, H. Heise, DNP-enhanced solid-state NMR at cryogenic temperatures: a tool to snapshot conformational ensembles of α-synuclein in different states, Biophys. J. 114 (7) (2018) 1614–1623, https://doi.org/10.1016/j.bpj.2018.02.011.
* Our study representing different αS conformational ensembles simultaneously. Broad-peaks are not always bad !, but may contain valuable information when tackled correctly.
[105] K.-N. Hu, R.H. Havlin, W.-M. Yau, R. Tycko, Quantitative determination of site-specific conformational distributions in an unfolded protein by solid-state nuclear magnetic resonance, J. Mol. Biol. 392 (4) (2009) 1055–1073.
[106] (*) S. Lange, W.T. Franks, N. Rajagopalan, K. Döring, M.A. Geiger, A. Linden, B.-J. van Rossum, G. Kramer, B. Bukau, H. Oschkinat, Structural analysis of a signal peptide inside the ribosome tunnel by DNP MAS NMR, Sci. Adv. 2 (8) (2016).
* A study of signal-peptide in intact ribosome tunnel, showing the pre-secreted protein conformations. A beautiful model system representing the uniqueness of DNP NMR approach.
[107] Y. Geiger, H.E. Gottlieb, U. Akbey, H. Oschkinat, G. Goobes, Studying the conformation of a silaffin-derived pentalysine peptide embedded in bioinspired silica using solution and dynamic nuclear polarization magic-angle spinning NMR, J. Am. Chem. Soc. 138 (17) (2016) 5561–5567.

[108] M. Hong, K. Jakes, Selective and extensive 13C labeling of a membrane protein for solid-state NMR investigations, J. Biomol. NMR 14 (1) (1999) 71–74.
[109] H. Heise, W. Hoyer, S. Becker, O.C. Andronesi, D. Riedel, M. Baldus, Molecular-level secondary structure, polymorphism, and dynamics of full-length α-synuclein fibrils studied by solid-state NMR, Proc. Natl. Acad. Sci. U.S.A. 102 (44) (2005) 15871–15876.
[110] T. Viennet, M.M. Wördehoff, B. Uluca, C. Poojari, H. Shaykhalishahi, D. Willbold, B. Strodel, H. Heise, A.K. Buell, W. Hoyer, M. Etzkorn, Structural insights from lipid-bilayer nanodiscs link α-Synuclein membrane-binding modes to amyloid fibril formation, Commun. Biol. 1 (1) (2018) 44.
[111] (*) A. Potapov, W.M. Yau, R. Ghirlando, K.R. Thurber, R. Tycko, Successive stages of amyloid-beta self-assembly characterized by solid-state nuclear magnetic resonance with dynamic nuclear polarization, J. Am. Chem. Soc. 137 (25) (2015) 8294–8307.
* A nice example of DNP NMR study on Aβ fibrils. Extends structural information towards different stages of fibrillation process.
[112] M. Kaplan, A. Cukkemane, G.C. van Zundert, S. Narasimhan, M. Daniels, D. Mance, G. Waksman, A.M. Bonvin, R. Fronzes, G.E. Folkers, M. Baldus, Probing a cell-embedded megadalton protein complex by DNP-supported solid-state NMR, Nat. Methods 12 (7) (2015) 649–652.
[113] M. Kaplan, S. Narasimhan, C. de Heus, D. Mance, S. van Doorn, K. Houben, D. Popov-Celeketic, R. Damman, E.A. Katrukha, P. Jain, W.J. Geerts, A.J. Heck, G.E. Folkers, L.C. Kapitein, S. Lemeer, P.M. van Bergen En Henegouwen, M. Baldus, EGFR dynamics change during activation in native membranes as revealed by NMR, Cell 167 (5) (2016), 1241-1251 e11.
[114] T. Jacso, W.T. Franks, H. Rose, U. Fink, J. Broecker, S. Keller, H. Oschkinat, B. Reif, Characterization of membrane proteins in isolated native cellular membranes by dynamic nuclear polarization solid-state NMR spectroscopy without purification and reconstitution, Angew. Chem., Int. Ed. Engl. 51 (2) (2012) 432–435.
[115] M. Renault, S. Pawsey, M.P. Bos, E.J. Koers, D. Nand, R. Tommassen-van Boxtel, M. Rosay, J. Tommassen, W.E. Maas, M. Baldus, Solid-state NMR spectroscopy on cellular preparations enhanced by dynamic nuclear polarization, Angew. Chem., Int. Ed. Engl. 51 (12) (2012) 2998–3001.
[116] K. Yamamoto, M.A. Caporini, S.C. Im, L. Waskell, A. Ramamoorthy, Cellular solid-state NMR investigation of a membrane protein using dynamic nuclear polarization, Biochim. Biophys. Acta 1848 (1 Pt B) (2015) 342–349.
[117] B.J. Albert, C. Gao, E.L. Sesti, E.P. Saliba, N. Alaniva, F.J. Scott, S.T. Sigurdsson, A.B. Barnes, Dynamic nuclear polarization nuclear magnetic resonance in human cells using fluorescent polarizing agents, Biochemistry 57 (31) (2018) 4741–4746.
[118] E. Luchinat, L. Banci, In-cell NMR: a topical review, IUCrJ 4 (2) (2017) 108–118.
[119] D.J. Kubicki, G. Casano, M. Schwarzwälder, S. Abel, C. Sauvée, K. Ganesan, M. Yulikov, A.J. Rossini, G. Jeschke, C. Copéret, A. Lesage, P. Tordo, O. Ouari, L. Emsley, Rational design of dinitroxide biradicals for efficient cross-effect dynamic nuclear polarization, Chem. Sci. 7 (1) (2016) 550–558.
[120] E. Ravera, C. Luchinat, G. Parigi, Basic facts and perspectives of Overhauser DNP NMR, J. Magn. Reson. 264 (2016) 78–87.
[121] U. Akbey, W.T. Franks, A. Linden, S. Lange, R.G. Griffin, B.J. van Rossum, H. Oschkinat, Dynamic nuclear polarization of deuterated proteins, Angew. Chem. Int. Ed. 49 (42) (2010) 7803–7806.
[122] M.A. Geiger, M. Orwick-Rydmark, K. Marker, W.T. Franks, D. Akhmetzyanov, D. Stoppler, M. Zinke, E. Specker, M. Nazare, A. Diehl, B.J. van Rossum, F. Aussenac, T. Prisner, U. Akbey, H. Oschkinat, Temperature dependence of cross-effect dynamic nuclear polarization in rotating solids: advantages of elevated temperatures, Phys. Chem. Chem. Phys. 18 (44) (2016) 30696–30704.
[123] E.P. Saliba, E.L. Sesti, F.J. Scott, B.J. Albert, E.J. Choi, N. Alaniva, C. Gao, A.B. Barnes, Electron decoupling with dynamic nuclear polarization in rotating solids, J. Am. Chem. Soc. 139 (18) (2017) 6310–6313.
[124] T. Maly, G.T. Debelouchina, V.S. Bajaj, K.N. Hu, C.G. Joo, M.L. Mak-Jurkauskas, J.R. Sirigiri, P.C.A. van der Wel, J. Herzfeld, R.J. Temkin, R.G. Griffin, Dynamic nuclear polarization at high magnetic fields, J. Chem. Phys. 128 (5) (2008), 052211.
[125] G. Mathies, S. Jain, M. Reese, R.G. Griffin, Pulsed dynamic nuclear polarization with trityl radicals, J. Phys. Chem. Lett. 7 (1) (2016) 111–116.